

Conduction Mechanism in a Molecular Hydrogen Contact

K. S. Thygesen and K. W. Jacobsen
*Center for Atomic-scale Materials Physics,
Department of Physics, Technical University of Denmark,
DK - 2800 Kgs. Lyngby, Denmark*
(Dated: November 18, 2018)

We present first principles calculations for the conductance of a hydrogen molecule bridging a pair of Pt electrodes. The transmission function has a wide plateau with $T \approx 1$ which extends across the Fermi level and indicates the existence of a single, robust conductance channel with nearly perfect transmission. Through a detailed Wannier function analysis we show that the H_2 bonding state is not involved in the transport and that the plateau forms due to strong hybridization between the H_2 anti-bonding state and states on the adjacent Pt atoms. The Wannier functions furthermore allow us to derive a resonant-level model for the system with all parameters determined from the fully self-consistent Kohn-Sham Hamiltonian.

PACS numbers: 73.63.Rt, 73.20.Hb, 73.40.Gk

The study of electron transport through single molecules has evolved during the last decade as new experimental techniques have made it possible to produce atomic-scale contacts with a few or even a single molecule suspended between macroscopic electrodes [1, 2, 3, 4]. At the same time theoretical efforts have been made to describe and understand the experiments from first principles [5, 6, 7]. The connection between experiment and theory, however, has been complicated by the crucial but in practice uncontrollable atomistic details of the contact region between the molecule and the leads. While the majority of previously investigated molecules have shown a conductance much lower than the quantum unit, $G_0 = 2e^2/h$, Smit. *et al.* recently measured a conductance close to $1G_0$ for a hydrogen molecule bridging a pair of Pt electrodes [8]. The result immediately raises the question: how can a hydrogen molecule which has a closed shell configuration and a large energy gap be conducting? Despite the simplicity of the system, there are still considerable disagreements among the reported calculations for the conductance of the hydrogen bridge. Quantitatively, values of $0.9G_0$ [8, 9] and $(0.2 - 0.5)G_0$ [10] have been published by different groups using similar methods. Perhaps even more importantly, the physical explanations for the obtained results are very different. Indeed, both the bonding [9, 10] as well as the anti-bonding [8] state of the H_2 molecule have been proposed as the current-carrying state.

In this letter we present conductance calculations based on Density Functional Theory (DFT) showing that a hydrogen molecule bridging a pair of Pt contacts can have a conductance close to $1G_0$ and we explain the physical mechanism behind this result. The transmission function is found to have a characteristic plateau with $T \approx 1$ in an energy window of 4 eV around the Fermi level, indicating the existence of a single, very robust conductance channel with nearly perfect transmission. By performing a Wannier function (WF) analysis

we can directly study the transmission through the H_2 bonding and anti-bonding states separately. The results clearly demonstrate that the bonding state takes almost no part in the transport and that the plateau is a result of a strong hybridization between the H_2 anti-bonding state and a combination of d - and s -like orbitals located on the neighboring Pt atoms. The analysis furthermore allows us to determine characteristic model parameters from first principles which in turn provides a very simple description of the system.

To describe the molecular contact we use the supercell shown in the inset of Fig. 1. It contains the H_2 molecule anchored between two 4-atom Pt pyramids which again are attached to Pt(111) surfaces [11]. We calculate the conductance of the relaxed structures assuming that the electrons move phase coherently through the contact and are influenced only by the self-consistent Kohn-Sham potential. In this case the conductance is given by $G = G_0 T(\varepsilon_F)$, where $T(\varepsilon_F)$ is the transmission function at the Fermi level [15]. The transmission function is found using the Green's function method described in Refs. [16, 17, 18]. In this approach the system is divided into three regions: A left lead, L , a right lead, R , and a central region, C . The leads are assumed to be periodic such that all scattering takes place in C . In our case C coincides with the supercell of the DFT calculation and the leads are bulk Pt(fcc) described in a supercell containing 3×3 atoms in the transverse plane to match the central region at the interfaces. The transmission function is then given by the formula [19]

$$T(\varepsilon) = \text{Tr}[G_C^r(\varepsilon)\Gamma_L(\varepsilon)G_C^a(\varepsilon)\Gamma_R(\varepsilon)], \quad (1)$$

where G_C^r is the retarded Green's function of the scattering region

$$G_C^r(\varepsilon) = [(\varepsilon + i\eta^+)S - \Sigma_L(\varepsilon) - \Sigma_R(\varepsilon) - H_C]^{-1}. \quad (2)$$

Here H_C and S are the Hamiltonian and overlap matrices of the central region, η^+ is a positive infinitesimal and Σ_α

is the self-energy from lead α . The coupling strength of lead α is given by $\Gamma_\alpha = i(\Sigma_\alpha - \Sigma_\alpha^\dagger)$.

We use partly occupied Wannier functions, $\{\phi_{n\alpha}\}$, (see below) as basis functions in each of the three regions ($\alpha = L, R, C$). Due to the limited size of the supercell in the plane perpendicular to the transport direction the conductance should be calculated as an integral over the Brillouin zone in the corresponding plane. We thus form the Bloch states $\psi_{\mathbf{k}_\perp n\alpha}(\mathbf{r}) = \sum_{\mathbf{R}_\perp} e^{i\mathbf{k}_\perp \cdot \mathbf{R}_\perp} \phi_{n\alpha}(\mathbf{r} - \mathbf{R}_\perp)$, where \mathbf{R}_\perp runs over supercells in the transverse plane. For each \mathbf{k}_\perp we obtain a Hamiltonian matrix $H(\mathbf{k}_\perp)_{n\alpha, m\beta} = \langle \mathbf{k}_\perp n\alpha | H | \mathbf{k}_\perp m\beta \rangle$ which in turn leads to a conductance $G(\mathbf{k}_\perp)$ through Eq. (1). The integrated conductance can then be approximated by the finite sum $\sum_{\mathbf{k}_\perp} w(\mathbf{k}_\perp) G(\mathbf{k}_\perp)$, where $w(\mathbf{k}_\perp)$ are appropriate weight factors.

We focus on a single, fully relaxed contact characterized by the bond lengths $d_{\text{H-H}} = 1.0 \text{ \AA}$ and $d_{\text{Pt-H}} = 1.76 \text{ \AA}$. The vibrational modes of the hydrogen molecule in this configuration are in fair agreement with new experimental results [20]. In Fig. 1 we show the transmission function calculated using 8 irreducible \mathbf{k} -points to sample the transverse BZ. The same curve calculated within the widely used Γ -point approximation is shown for comparison. The two curves have essentially the same features, however, the Γ -point curve has more structure. This is because the \mathbf{k} -point sampling provides the correct smearing of the electronic structure in the leads which effectively washes out features related to single points in the transverse plane of the lead Brillouin zone. An in-

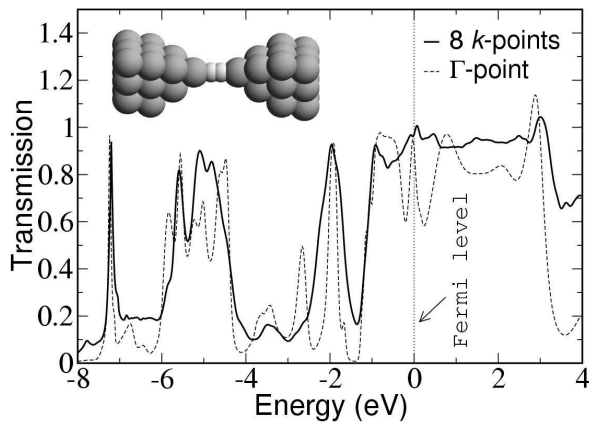


FIG. 1: Calculated transmission for the molecular hydrogen contact shown in the inset. For comparison both the \mathbf{k} -point sampled transmission and the Γ -point transmission are shown. The Γ -point transmission has more structure, however, the qualitative features of the curves are essentially the same. The wide plateau with $T \approx 1$ extending across the Fermi level indicates a single, very robust conductance channel with nearly perfect transmission.

teresting feature of the transmission function is the wide plateau with $T \approx 1$ extending across the Fermi level. We shall refer to this plateau as the $1G_0$ -plateau.

To gain insight into the formation of the $1G_0$ -plateau we perform a Wannier function analysis. The WFs are defined as linear combinations of the Kohn-Sham eigenstates with the expansion coefficients chosen to make the WFs orthogonal and maximally localized. By including selected unoccupied eigenstates in this construction we can obtain good localization properties of the WFs also for metallic systems [21, 22]. We stress that the minimal WF basis set retains the accuracy of the plane wave DFT calculation since the WFs by construction span the eigenstates below a certain energy which has been set to 4 eV above the Fermi level in the present calculation. The transformation results in the following set of WFs: For each Pt we obtain 5 d -orbitals centered at the atom and a single σ -orbital located at an interstitial site. For each hydrogen we find an s -orbital, $|i\rangle$ ($i = 1, 2$), which is slightly elongated towards the contacting Pt atom. We proceed by transforming the hydrogen s -orbitals into bonding and anti-bonding combinations $|b\rangle = (|1\rangle + |2\rangle)/\sqrt{2}$ and $|a\rangle = (|1\rangle - |2\rangle)/\sqrt{2}$. $|a\rangle$ and $|b\rangle$ are the only states with significant weight on the molecule and provide two conductance channels well separated in energy. The on-site energies are $\langle b | H | b \rangle = -6.4 \text{ eV}$ and $\langle a | H | a \rangle = 0.1 \text{ eV}$ relative to the Fermi level of the metal. By cutting all coupling matrix elements involving the bonding, respectively, the anti-bonding state we can directly test their individual contributions to the total conductance when interference

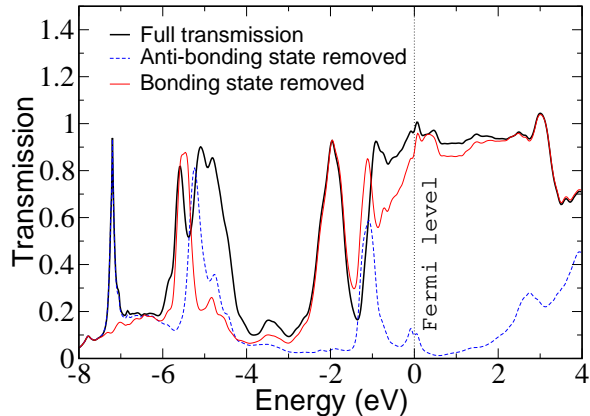


FIG. 2: Calculated transmission for the structure shown in the inset of Fig. 1 when all coupling to the bonding, respectively, the anti-bonding H_2 state has been cut. The full transmission has been repeated for comparison. The narrow peak around -7 eV is clearly due to the bonding state, while the peak at -2 eV and the wide plateau around the Fermi level almost exclusively involve the anti-bonding state.

is neglected. The result is shown in Fig. 2. The narrow peak just below -7 eV is completely gone when the bonding state is removed but is not affected by the absence of the anti-bonding state. The peak is thus clearly due to transmission through the bonding channel which is in good agreement with the calculated on-site energy of $|b\rangle$. In the energy regime $-6 - 4$ eV both the bonding and anti-bonding states contribute to the transmission. For energies above -3 eV the removal of the bonding state has little effect on the transmission which must therefore be ascribed to the anti-bonding state. A small exception to this is the narrow peak at -1 eV which is caused by hybridization of the bonding state with Pt d_{z^2} -orbitals on the contacting atoms. Overall we can conclude that the peak at -2 eV and the $1G_0$ -plateau which determines the conductance are due to transmission through the anti-bonding state.

The fact that the bonding state takes almost no part in the transmission around the Fermi level allows us to describe the contact by a resonant level model [23] with all parameters determined from first principles. In the resonant level model we consider a single level, $|a\rangle$, of energy $\varepsilon_a = \langle a|H|a\rangle$ coupled to infinite leads via the matrix elements $t_{k\alpha} = \langle k\alpha|H|a\rangle$, where $\{|k\alpha\rangle\}$ is a basis of lead α . The model has served as starting point for many more advanced studies such as shot noise, electron-electron and electron-phonon interactions in resonant tunneling systems [24, 25, 26]. A particularly useful formulation of the model can be obtained if we introduce the group orbital of lead α by $|g_\alpha\rangle = c_\alpha P_\alpha H|a\rangle$, where P_α is the orthogonal projection onto lead α and c_α is a normalization constant. By supplementing the group orbital by orthonormal states $\{|\tilde{k}\alpha\rangle\}$ we obtain a new basis with the key property $\langle \tilde{k}\alpha|H|a\rangle = 0$ for all \tilde{k} . The level is thus coupled to the lead via the group orbital only. Since the

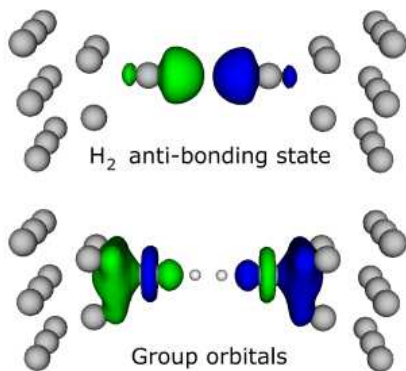


FIG. 3: Contour plots of the orbitals determining the transport properties of the hydrogen contact: the H_2 anti-bonding state, $|a\rangle$, and the corresponding left and right group orbitals, $|g_L\rangle, |g_R\rangle$. The left (right) group orbital has been constructed by applying the DFT Hamiltonian to $|a\rangle$ and then projecting onto the Wannier functions of the left (right) part of the contact.

contact is symmetric $\langle g_L|H|a\rangle = \langle g_R|H|a\rangle \equiv V$. The imaginary part of the level self-energy, Δ_a , is directly related to the DOS of the group orbitals calculated with $V = 0$: $\Delta_a = \pi|V|^2(\rho_L^0 + \rho_R^0) = (\Gamma_L + \Gamma_R)/4$. The real part of the self-energy is the Hilbert transform of Δ_a . For a symmetric contact we have $\rho_L^0 = \rho_R^0 \equiv \rho_g^0$ and the transmission in Eq. (1) takes the simple form

$$T(\varepsilon) = 2\pi^2|V|^2\rho_g^0(\varepsilon)\rho_a(\varepsilon). \quad (3)$$

Since ρ_a can be obtained from Σ_a and ε_a this expression shows that the transmission is determined by the three quantities ρ_g^0 , V and ε_a .

By applying the DFT Hamiltonian to $|a\rangle$ in the WF basis we construct the group orbitals of the H_2 anti-bonding state. Contour plots of the orbitals are shown in Fig. 3. The group orbital is mainly composed of the d_{z^2} -orbital of the apex Pt atom and three σ -orbitals centered within the Pt pyramid. We calculate ρ_g^0 for the uncoupled system by cutting all coupling matrix elements to $|a\rangle$. The result is shown in the upper panel of Fig. 4 together with ρ_a and the transmission function. The pronounced peak at -1 eV is due to the d_{z^2} -orbitals on the apex Pt atoms.

If we neglect the narrow peak at -1 eV, ρ_g^0 can be described by a semi-elliptical band on top of a flat background, see lower panel of Fig. 4. The coupling and level energy can be directly read off the Hamiltonian matrix and we find $V = 1.9$ eV and $\varepsilon_a = 0.1$ eV relative to the Fermi level. It should be noticed that the coupling which is relevant for the adsorption of the hydrogen molecule to the contact is $\sqrt{2}V = 2.7$ eV since the level is coupled

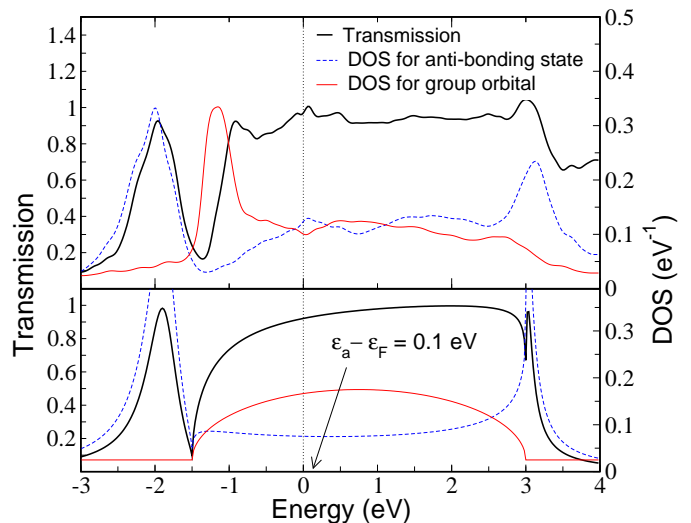


FIG. 4: Upper panel shows the transmission together with the projected density of states (DOS) for the H_2 anti-bonding state and the corresponding left group orbital. The lower panel shows the same quantities obtained from the single-level model when ρ_g^0 is approximated by a semi-elliptical band and we use the coupling, V , and on-site energy, ε_a , from the first principles calculation.

by V to *both* leads. From these parameters we can determine the Green's function for the level which in turn yields ρ_a and T . The result is summarized in the lower panel of Fig. 4. Based on the good agreement with the first principles results we conclude that the simple model indeed gives a realistic description of the system. It is then clear that the peak at -2 eV represents the bonding combination between $|a\rangle$ and the Pt band and that the $1G_0$ -plateau forms because: (i) ε_a lies close to the Fermi level and well inside the relevant Pt band as defined by the group orbital. (ii) the width of the renormalized level (Δ_a) is comparable to the band width, i.e. the limit of strong chemisorption [23].

The crucial point in the proposed mechanism is the strong hybridization of the H_2 anti-bonding state with the Pt bands around the Fermi level. This picture agrees well with the conventional understanding of hydrogen dissociation on simple and transition metal surfaces which has been established on the basis of DFT calculations [27, 28]. The bonding and antibonding states of a hydrogen molecule at a simple metal surface are broadened and furthermore shifted down due to the hybridization with the metal s - and p -states. During the dissociation process the antibonding resonance crosses the Fermi level and becomes gradually filled with the result that the hydrogen-hydrogen bond is weakened. For the transition metal the same general picture applies, but the hybridization with the d -states further affects the antibonding resonance. The fact that the antibonding state in the calculations for the bridging hydrogen molecule between Pt contacts is close to the Fermi level is thus an indication that the hydrogen-hydrogen bond is weakened by the coupling to the metal in agreement with the resulting increase of the hydrogen-hydrogen bond length. The values we find for the positions of the bonding and antibonding molecular levels, $\varepsilon_b = -6.4$ eV, $\varepsilon_a = 0.1$ eV are in fact quite close to the ones used by Hammer and Nørskov [27] ($\varepsilon_b = -7$ eV, $\varepsilon_a = 1$ eV) to describe hydrogen in the dissociative transition state on metals. This is in clear contrast to the studies by Cuevas *et al.* [9] and García *et al.* [10] who consider the hydrogen molecule in the bridging position to have almost the same bond length as the free molecule and who report very large bonding-antibonding splittings of 23-24 eV which even exceed the DFT-PW91 value of 10.4 eV for a free molecule.

In summary, we have presented first principles conductance calculations showing that a hydrogen molecule suspended between Pt contacts can have a conductance close to $1G_0$. Through a detailed Wannier function analysis we have identified the conduction mechanism as being due to a strong hybridization between the H_2 anti-bonding state and certain Pt bands. A resonant level model with all parameters determined from the self-consistent DFT Hamiltonian was shown to account for the important features of the first principles transmission function.

We would like to thank J. van Ruitenbeek and D. Djukic for many inspiring discussions. We acknowledge support from the Danish Center for Scientific Computing through Grant No. HDW-1101-05.

mic for many inspiring discussions. We acknowledge support from the Danish Center for Scientific Computing through Grant No. HDW-1101-05.

-
- [1] C. Joachim, J. K. Gimzewski, R. R. Schlittler and C. Chavy Phys. Rev. Lett. **74**, 2102 (1995).
 - [2] M. A. Reed, C. Zhou, C. J. Muller, T. P. Burgin and J. M. Tour Science **278**, 252 (1997).
 - [3] J. Reichert, R. Ochs, D. Beckman, H. B. Weber, M. Mayor and H. v. Löhneysen Phys. Rev. Lett. **88**, 176804 (2002).
 - [4] B. Xu and N. J. Tao Science **301**, 1221 (2003).
 - [5] J. Taylor, M. Brandbyge and K. Stokbro Phys. Rev. Lett. **89**, 138301 (2002).
 - [6] P. S. Damle, A. W. Ghosh and S. Datta Phys. Rev. B **64**, 201403 (2001).
 - [7] M. Di Ventra, S. T. Pantelides and N. D. Lang Phys. Rev. Lett. **88**, 046801 (2002).
 - [8] R. H. M. Smit, Y. Noat, C. Untiedt, N. D. Lang, M. C. van Hemert and J. M. van Ruitenbeek, Nature **419**, 906 (2002).
 - [9] J. C. Cuevas, J. Heurich, F. Pauly, W. Wenzel, and G. Schön, Nanotechnology, **14**, R29 (2003).
 - [10] Y. García, J. J. Palacios, E. SanFabián, J. A. Vergés, A. J. Pérez-Jiménez and E. Louis, Phys. Rev. B **69**, 041402(R) (2004).
 - [11] The surface is modeled as a slab with a thickness of 4 atomic layers and the supercell contains 3×3 atoms in the surface plane. Both the Pt pyramids and the H atoms have been relaxed using a plane wave DFT code [12] to obtain the most stable contact geometry. We use an energy cut-off of 25 Ry for the plane wave expansion and describe the ion cores by ultrasoft pseudopotentials [13]. To treat exchange and correlation we use the PW91 functional [14]. The Brillouin zone is sampled by a single \mathbf{k} -point along the contact axis (z -axis) and 4×4 \mathbf{k} -points in the transverse plane.
 - [12] B. Hammer, L.B. Hansen, and J.K. Nørskov, Phys. Rev. B **59**, 7413 (1999); S.R. Bahn and K.W. Jacobsen, Comp. Sci. Eng. **4**, 56 (2002); The Dacapo code can be downloaded at <http://www.fysik.dtu.dk/campos>.
 - [13] D. Vanderbilt, Phys. Rev. B **41**, 7892 (1990).
 - [14] J. P. Perdew, J. A. Chevary, S. H. Vosko, K. A. Jackson, M. R. Pederson, D. J. Singh and C. Fiolhais, Phys. Rev. B **46**, 6671 (1992).
 - [15] S. Datta, *Electronic Transport in Mesoscopic Systems* Cambridge (1995).
 - [16] K. S. Thygesen, M. V. Bollinger and K. W. Jacobsen, Phys. Rev. B **67**, 115404 (2003).
 - [17] Y. Xue, S. Datta and M. A. Ratner Chem. Phys. **281**, 151 (2002)
 - [18] M. Brandbyge, J. L. Mozos, P. Ordejón, J. Taylor and K. Stokbro Phys. Rev. B **65**, 165401 (2002).
 - [19] Y. Meir and N. S. Wingreen, Phys. Rev. Lett. **68**, 2512 (1992).
 - [20] D. Djukic and J. M. van Ruitenbeek, private communication
 - [21] I. Souza, N. Marzari and D. Vanderbilt, Phys. Rev. B **65**, 035109 (2001).
 - [22] K. S. Thygesen and K. W. Jacobsen,

arXiv:cond-mat/0411086.

- [23] D. M. Newns, Phys. Rev. **178**, 1123 (1969).
- [24] A. Thielmann, M. H. Hettler, J. König and G. Schön Phys. Rev. B **68**, 115105 (2003).
- [25] T. K. Ng and P. A. Lee Phys. Rev. Lett. **61**, 1768 (1988).
- [26] P. Hyldgaard, S. Hershfield, J. H. Davies and J. W. Wilkins Ann. Phys. **236**, 1 (1994).
- [27] B. Hammer and J. K. Nørskov, Surface Science **343**, 211 (1995).
- [28] J. K. Nørskov, A. Houmøller, P. K. Johansson and B. I. Lundqvist, Phys. Rev. Lett. **46**, 257 (1981).